PHYSICAL REVIEW B **83**, 220301(R) (2011)

Strontium migration assisted by oxygen vacancies in $SrTiO_3$ from classical and quantum mechanical simulations

Aron Walsh,[1,*] C. Richard A. Catlow,[2] Alastair G. H. Smith,[2] Alexey A. Sokol,[2] and Scott M. Woodley[2]

[1]*Centre for Sustainable Chemical Technologies and Department of Chemistry, University of Bath, Claverton Down, Bath BA2 7AY, United Kingdom*

[2]*University College London, Kathleen Lonsdale Materials Chemistry, Department of Chemistry, 20 Gordon Street, London WC1H 0AJ, United Kingdom*

(Received 10 February 2011; revised manuscript received 14 March 2011; published 3 June 2011)

We present the pathways for strontium ion migration in $SrTiO_3$, which are based on an exploration of the potential energy landscape through a combination of classical and quantum mechanical techniques. Sr ion migration is enhanced by interaction with an anion vacancy: In the bulk material, Sr cations migrate linearly between adjacent lattice sites, through the center of a square formed by four oxygen ions; however, the activation barrier is substantially reduced, and the path curved, in the presence of an oxygen vacancy. The contribution of partial Schottky disorder in the SrO sublattice to ion migration explains the wide spread of experimental results to date, with direct implications for diffusion processes at highly doped surfaces and interfaces of $SrTiO_3$ as well as other perovskite materials.

DOI: 10.1103/PhysRevB.83.220301 PACS number(s): 66.30.Lw, 61.72.J−, 77.84.Bw

Ternary ABO_3 metal oxides adopting the perovskite crystal structure are known for their rich physical properties ranging from electrically semiconducting to superconducting behavior, in addition to being prototypal ferroelectric ceramics.[1–3] $SrTiO_3$ is a perovskite material that exhibits a combination of electronic and ionic conductivity, both of which are determined by the underlying defect chemistry of the material.[4] These unique properties are intimately related to the high-mobility electron gas formed at $SrTiO_3$ interfaces[5,6] and surfaces,[7,8] and to its application as a photocatalyst.[9] Recently, $SrTiO_3$ has been the subject of a study for random access memory, where ion mobility is critical for achieving resistance-switching behavior.[10,11]

In $SrTiO_3$, oxygen loss is associated with a chemical reduction of titanium, and the oxygen ion diffusion process has attracted significant attention:[12–14] In the bulk material, oxygen diffusion is a vacancy mediated low-energy process ($E_{act} \sim$ 1 eV, excluding the defect formation energy), following a curved path around the neighboring titanium cation, rather than a linear ⟨110⟩ direct path, between two oxygen lattice sites.[15–17] Cation migration is also known to occur,[18,19] but the process is not fully understood. In this Rapid Communication, we present a computational investigation of the energy landscape for Sr migration: While the pathway between two Sr sites is linear in the bulk material, the presence of an oxygen vacancy effects a curved path along with a reduction of 0.76 eV in the activation energy for ion migration.

The stable room-temperature phase of $SrTiO_3$ is the cubic perovskite structure. At lower temperatures, perovskite materials typically undergo a series of phase transitions, which involve rotations and tilting of the TiO_6 octahedra producing tetragonal, possibly orthorhombic, and eventually rhombohedral crystal structures.[20–24] This sequence is predicted by our *ab initio* calculations using energy minimization techniques. However, only the tetragonal phase is in fact observed experimentally below 105 K, whereas the exact nature of the lower-temperature phenomena is still under debate. The nature of all such transitions has been well studied for another perovskite material—$BaTiO_3$.[25–28] The nature of the low-temperature behavior and stabilization of the tetragonal structure of $SrTiO_3$ is beyond the scope of the current investigation. The structural changes involved in these phase transitions are very small and will have only a minor effect on the relatively high-energy defect formation and migration processes. Hence in this study, we choose to model the minimum energy rhomohedral perovskite phase of $SrTiO_3$, as shown in Fig. 1, where no imaginary phonon modes were present—as confirmed explicitly through density functional perturbation theory calculations—which avoid the spurious effects of a partial phase transition on defect formation or ion transport.

Classical interatomic potential calculations were used to explore the energy hypersurface for oxygen vacancy and cation migration (see examples in Fig. 2), with the energy barriers obtained using an electronic structure approach. The combination of these two approaches allows for a comprehensive sampling of possible diffusion pathways, while providing quantitative estimates of the barriers for diffusion that represent the predominant contribution to observable rates. For the former calculations, a polarizable interatomic potential model[29] was employed, which was recently developed to reproduce the structural, elastic, and dielectric properties of $SrTiO_3$; all calculations were performed within the primary code GULP[30] and the auxiliary codes PREGULP[31,32] and BUBBLE.[33,34] More accurate quantum mechanical calculations were performed at the level of density functional theory (DFT) within the generalized gradient approximation (PBEsol functional[35]) in the code VASP.[36–38] To obtain the barriers for ion migration, the transition states were probed via the nudged elastic band method in a pseudocubic 4×4×4 perovskite supercell of 320 atoms, with 18 images.[39] In $SrTiO_3$, the occupied valence states at the top of the valence band are strongly localized on the oxygen sublattice, while the unoccupied conduction states are localized on Ti at the bottom of the conduction band, and Sr higher up. Due to the underestimated band gap at this level of DFT, anion polarization is overestimated, which will result

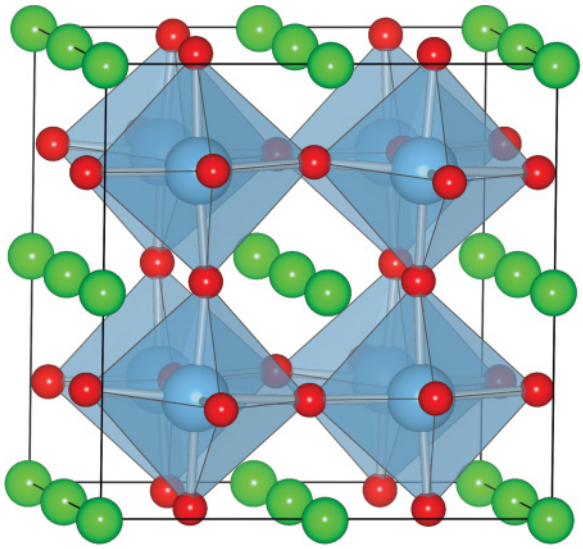

FIG. 1. (Color online) Representation of the rhombohedral perovskite phase of $SrTiO_3$ as a 2×2×2 pseudocubic supercell. Note the small tilting of the TiO_6 octahedra, which is not present in the high-temperature cubic perovskite structure. The titanium octahedra are shaded blue (gray), with oxygen atoms colored red (small balls).

in an *underestimation* of the barrier height for oxygen ion migration; however, for Sr migration, this is counterbalanced by the increase in the self-interaction as the electrons displace toward the Sr ion at the saddle point, thus some *overestimation* for strontium may be expected.

The pertinent migration pathways explored are summarized in Fig. 3. For oxygen ion migration, we observe a curved path, as shown in Fig. 2(a), which is consistent with the accepted model for perovskite materials.[17,40–42] Curiously, we have observed that in the absence of structural relaxation, the saddle point is in fact a local minimum of the potential energy surface. On relaxation, the calculated migration energy of 0.53 eV is comparable to values ranging from 0.65 to 1.35 eV, obtained using interatomic potential models,[29] and to 0.65–1.27 eV based on experimental measurements.[43,44] From diffusion measurements in single-crystal samples of $SrTiO_3$, the lower values were observed in samples with higher dislocation densities,[44] which strongly suggests that the upper values are more representative of the bulk material.

For strontium ion migration in the perfect material, i.e., where there are no oxygen vacancies, migration follows a linear path between neighboring lattice sites as shown in Fig. 3(c). The local coordination environment at the saddle point consists of a Sr ion in a square planar configuration with respect to oxygen, which is illustrated in Fig. 4(a). The calculated activation energy is 3.68 eV for migration, which compares to values of 2.5–4.3 eV obtained from classical modeling.[29] An experimental activation energy of 3.5 eV for Sr ion migration has been estimated from the correlation between Sr and O migration in ^{18}O tracer diffusion measurements,[18] while 2.8 eV was reported based on impedance spectroscopy of donor-doped samples.[45] Both our calculated results and the experimental data are inconsistent with an earlier reported value of 6.0 eV from diffusion measurements.[19]

The dominant form of ionic disorder in $SrTiO_3$ is known to be of the Schottky type, involving stoichiometric amounts of anion and cation vacancies.[4,29] Furthermore, it has been shown that partial Schottky formation involving V_{Sr} and V_O vacancies can be more easily achieved, as it avoids vacancies on the highly charged titanium sublattice,[15,47] i.e.,

$$Sr_{Sr} + O_O \rightarrow V''_{Sr} + V^{\bullet\bullet}_O + SrO(s).$$

The reaction energy for partial Schottky formation has been estimated to be as low as 1.7 eV per defect,[29] while the calculated energy of association is less than 0.1 eV due to the high dielectric screening. The question arises then as to the effect of this Schottky disorder on the thermodynamics of ion self-diffusion. The pathways for ion diffusion in the presence of point defects, which have been investigated, are summarized in Fig. 3. While for isolated ion diffusion, oxygen ions will diffuse at a much faster rate than strontium ions, remarkably, interaction between the point defects results in an opposing effect. For oxygen ion diffusion, interaction with a strontium vacancy results in a retarding effect, while strontium ion mobility through an oxygen vacancy is significantly enhanced. The activation energies increase from 0.53 to 0.89 eV (O ion) and decrease from 3.68 to 2.92 eV (Sr ion), respectively. The latter decrease agrees well with the spread in experimentally determined migration barriers.

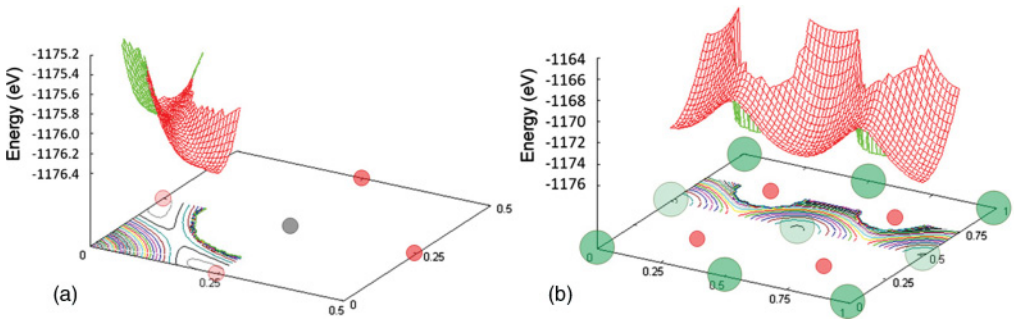

FIG. 2. (Color online) Isosurface and contours for key sections of the energy hypersurface for (a) oxygen ion migration in $SrTiO_{2.875}$ and (b) strontium ion migration in $Sr_{0.875}TiO_3$. Fractional coordinates refer to the pseudocubic supercell of rhombohedral perovskite phase of $SrTiO_3$ for the hypersurface and the 2×2×2 supercell of the cubic phase for the ionic coordinates of the spheres—red (small, light gray) oxygen, gray (small, dark gray) titanium, and green (large) strontium. Vacancies are highlighted by use of greater transparency.

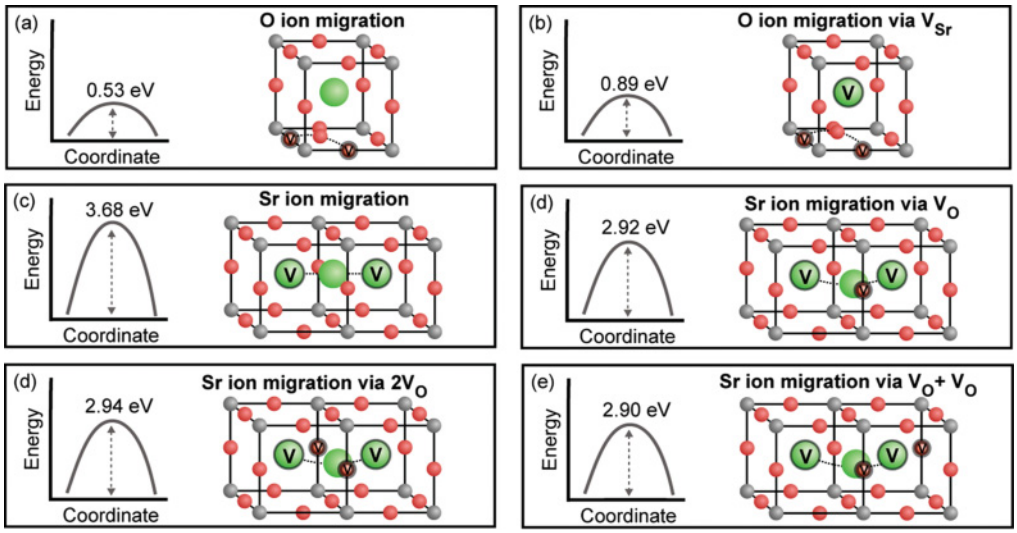

FIG. 3. (Color online) Schematic of the low-energy pathways predicted for Sr and O ion diffusion in $SrTiO_3$. The barrier heights were determined by first-principles calculations using the nudged elastic band method.

The structural configuration of the saddle point identified for Sr migration in the presence of an oxygen vacancy is shown in Fig. 4(b): In contrast to the square planar configuration for isolated ion migration, for this case, the Sr ion is displaced towards the vacancy site and the transition state is stabilized both by the increased Sr-O bond length, as well as through interaction with four additional oxygen ions in the vacancy plane (at a separation of ∼2.9 Å). Hence, a curved path is stabilized, which can allow for more rapid Sr ion migration. The frequency of ion "jumps" is determined by the standard rate equation, which has an exponential dependence on the free-energy barrier for ion migration. The change of 0.8 eV for Sr migration will therefore influence ion mobility by several orders of magnitude at standard temperatures.

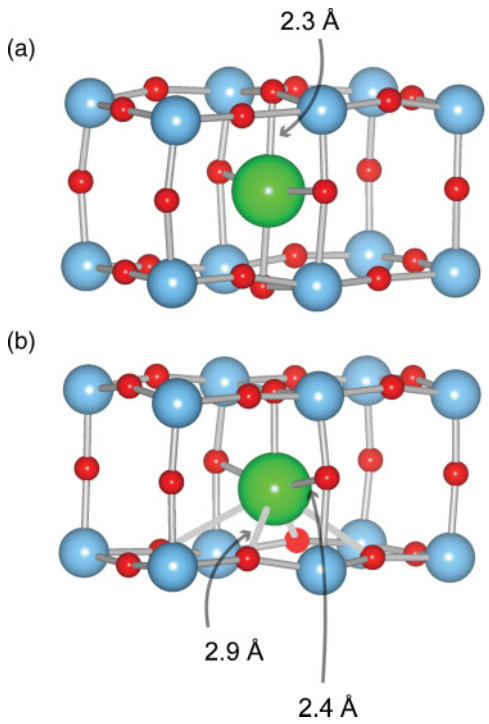

FIG. 4. (Color online) The local geometry associated with the transition state for Sr ion migration in (a) a bulk lattice and (b) in the presence of an oxygen vacancy, which have calculated activation energies for migration of 3.68 and 2.92 eV, respectively.

Due to the high dielectric screening of $SrTiO_3$, in the addition to the entropic barrier, association of the oppositely charged defects into bound complexes is not a source of concern. For example, an association energy of 0.05–0.01 eV has been calculated between strontium and oxygen vacancies,[29] which compares to 1.80 eV in In_2O_3.[32] In fact, the presence of additional oxygen vacancies does not affect the activation barrier for strontium mobility: In the vicinity of two oxygen vacancies, the activation energy is changed by less than 0.05 eV, irrespective of the relative vacancy orientation, and the migration path is largely unchanged from that of Fig. 4(b).

In conclusion, we have shown that Schottky disorder in $SrTiO_3$ can significantly affect ion transport, with a decrease in the barrier to Sr ion migration of 0.78 eV, which explains a spread in the experimentally determined migration barriers. Meanwhile, oxygen ion transport is retarded in the presence of a strontium vacancy, with an increase in the migration energy of 0.36 eV. The formation of charge accumulation layers at surface and interfaces of $SrTiO_3$ is associated with increased concentrations of point defects,[47] which would result in more frequent interactions and collisions between migrating ions and would also explain the scatter of experimentally determined activation energies for oxygen migration. The same situation could be observed for the case of extrinsic doping, where there will be a sensitive balance between electronic and ionic disorder.[48–50]

Thus, we have demonstrated that while complexation of oppositely charged defect centers is not anticipated in $SrTiO_3$ or other perovskite materials with high dielectric constants, the presence of stoichiometric defects can affect the fundamental thermodynamic quantities associated with ion transport. The interactions between point defects have a

direct implication in quantitative modeling of real material and devices, where contributions from Schottky disorder and reduction processes, particularly at material surfaces, grain boundaries, and dislocations must not be neglected.

We acknowledge support by an EPSRC Portfolio Partnership (Grant No. ED/D504872) and membership of the UK's HPC Materials Chemistry Consortium, which is funded by EPSRC (Grant No. EP/F067496).

*a.walsh@bath.ac.uk

[1] M. Choi, F. Oba, and I. Tanaka, Phys. Rev. Lett. **103**, 185502 (2009).
[2] J. F. Schooley, W. R. Hosler, and M. L. Cohen, Phys. Rev. Lett. **12**, 474 (1964).
[3] G. Borstel, E. A. Kotomin, R. I. Eglitis, and E. Heifets, Acta Phys. Pol. A **98**, 469 (2000).
[4] D. M. Smyth, *The Defect Chemistry of Metal Oxides* (Oxford University Press, Oxford, UK, 2000).
[5] J. M. Albina, M. Mrovec, B. Meyer, and C. Elsasser, Phys. Rev. B **76**, 165103 (2007).
[6] A. Ohtomo and H. Y. Hwang, Nature (London) **427**, 423 (2004).
[7] B. Meyer, J. Padilla, and D. Vanderbilt, Faraday Discuss. **114**, 395 (1999).
[8] W. Meevasana, P. D. C. King, R. H. He, S. K. Mo, M. Hashimoto, A. Tamai, P. Songsiriritthigul, F. Baumberger, and Z. X. Shen, Nat. Mater. **10**, 114 (2011).
[9] J. G. Mavroides, J. A. Kafalas, and D. F. Kolesar, Appl. Phys. Lett. **28**, 241 (1976).
[10] K. Szot, W. Speier, G. Bihlmayer, and R. Waser, Nat. Mater. **5**, 312 (2006).
[11] R. Waser and M. Aono, Nat. Mater. **6**, 833 (2007).
[12] X. D. Zhu, Y. Y. Fei, H. B. Lu, and G. Z. Yang, Appl. Phys. Lett. **87**, 051903 (2005).
[13] J. Claus, M. Leonhardt, and J. Maier, J. Phys. Chem. Solids **61**, 1199 (2000).
[14] P. Pasierb, S. Komornicki, and M. Rekas, J. Phys. Chem. Solids **60**, 1835 (1999).
[15] M. J. Akhtar, Z. U. N. Akhtar, R. A. Jackson, and C. R. A. Catlow, J. Am. Ceram. Soc. **78**, 421 (1995).
[16] J. Crawford and P. Jacobs, J. Solid State Chem. **144**, 423 (1999).
[17] M. Cherry, M. S. Islam, and C. R. A. Catlow, J. Solid State Chem. **118**, 125 (1995).
[18] R. Meyer, R. Waser, J. Helmbold, and G. Borchardt, Phys. Rev. Lett. **90**, 105901 (2003).
[19] W. H. Rhodes and W. D. Kingery, J. Am. Ceram. Soc. **49**, 521 (1966).
[20] A. Lebedev, Phys. Solid State **51**, 362 (2009).
[21] M. A. Saifi and L. E. Cross, Phys. Rev. B **2**, 677 (1970).
[22] W. G. Nilsen and J. G. Skinner, J. Chem. Phys. **48**, 2240 (1968).
[23] F. W. Lytle, J. Appl. Phys. **35**, 2212 (1964).
[24] R. Wahl, D. Vogtenhuber, and G. Kresse, Phys. Rev. B **78**, 104116 (2008).
[25] G. H. Kwei, A. C. Lawson, S. J. L. Billinge, and S. W. Cheong, J. Phys. Chem. **97**, 2368 (1993).
[26] B. Zalar, V. V. Laguta, and R. Blinc, Phys. Rev. Lett. **90**, 037601 (2003).
[27] M. I. Marques, Phys. Rev. B **71**, 174116 (2005).
[28] Q. Zhang, T. Cagin, and W. A. Goddard, Proc. Natl. Acad. Sci. (USA) **103**, 14695 (2006).
[29] C. R. A. Catlow, Z. X. Guo, M. Miskufova, S. A. Shevlin, A. G. H. Smith, A. A. Sokol, A. Walsh, D. J. Wilson, and S. M. Woodley, Philos. Trans. R. Soc. A **368**, 3379 (2010).
[30] J. D. Gale and A. L. Rohl, Mol. Simul. **29**, 291 (2003).
[31] PREGULP manages the input-output to and from GULP; creating input files, whereby the migrating ion is on one of the 64×64×64 grid points across the 2×2×2 pseudocubic supercell and the optimization flags are set so that the position of ions within 5 Å from either the migrating ion or the vacancy are relaxed during energy minimizations (which are performed by GULP).
[32] A. Walsh, S. M. Woodley, C. R. A. Catlow, and A. A. Sokol, Solid State Ionics **184**, 52 (2011).
[33] BUBBLE is used to analyze the energy hypersurface (i.e., to find the approximate migration pathways).
[34] S. M. Woodley and A. M. Walker, Mol. Simul. **33**, 1229 (2007).
[35] J. P. Perdew, A. Ruzsinszky, G. I. Csonka, O. A. Vydrov, G. E. Scuseria, L. A. Constantin, X. Zhou, and K. Burke, Phys. Rev. Lett. **100**, 136406 (2008).
[36] G. Kresse and J. Furthmüller, Phys. Rev. B **54**, 11169 (1996).
[37] G. Kresse and D. Joubert, Phys. Rev. B **59**, 1758 (1999).
[38] A plane-wave cutoff of 500 eV was employed.
[39] All point defects were treated in their formal oxidation states. Both explicit (point defects present within the supercell) and implicit (a homogeneous background charge) methods of charge compensation were found to produce equivalent migration barriers and local transition state geometries.
[40] A. V. Petrov, S. C. Parker, and A. Reller, Phase Transitions **55**, 229 (1995).
[41] S. M. Woodley, J. D. Gale, P. D. Battle, and C. R. A. Catlow, J. Chem. Phys. **119**, 9737 (2003).
[42] M. S. Islam, J. Mater. Chem. **10**, 1027 (2000).
[43] D. B. Schwarz and H. U. Anderson, J. Electrochem. Soc. **122**, 707 (1975).
[44] A. E. Paladino, L. G. Rubin, and J. S. Waugh, J. Phys. Chem. Solids **26**, 391 (1965).
[45] F. Poignant, Ph.D. thesis, Universite de Limoges, 1995.
[46] T. Tanaka, K. Matsunaga, Y. Ikuhara, and T. Yamamoto, Phys. Rev. B **68**, 205213 (2003).
[47] R. A. De Souza, J. Fleig, R. Merkle, and J. Maier, Z. Metallkd. **94**, 218 (2003).
[48] S. Saraf, M. Markovich, and A. Rothschild, Phys. Rev. B **82**, 245208 (2010).
[49] C. R. A. Catlow, A. A. Sokol, and A. Walsh, Chem. Comm. **47**, 3386 (2011).
[50] M. V. Raymond and D. M. Smyth, J. Phys. Chem. Solids **57**, 1507 (1996).